Bipotential adult liver progenitors are derived from chronically injured mature hepatocytes

Branden D. Tarlow[1,2,*], **Carl Pelz**[2], **Willscott E. Naugler**[3], **Leslie Wakefield**[2], **Elizabeth M. Wilson**[4], **Milton J. Finegold**[5], and **Markus Grompe**[2]

[1]Department of Cell, Developmental, and Cancer Biology, 3181 SW Sam Jackson Park Road, Portland, Oregon 97239, USA

[2]Department of Pediatrics, Oregon Health & Science University, 3181 SW Sam Jackson Park Road, Portland, Oregon 97239, USA

[3]Department of Gastroenterology & Hepatology, Oregon Health & Science University, 3181 SW Sam Jackson Park Road, Portland, Oregon 97239, USA

[4]Yecuris Corporation, PO BOX 4645, Tualatin, Oregon 97062, USA

[5]Department of Pathology, Baylor College of Medicine, 6621 Fannin St., Houston, Texas 77030, USA

Summary

Adult liver progenitor cells are biliary-like epithelial cells that emerge only under injury conditions in the periportal region of the liver. They exhibit phenotypes of both hepatocytes and bile ducts. However, their origin and their significance to injury repair remain unclear. Here, we used a chimeric lineage tracing system to demonstrate that hepatocytes contribute to the progenitor pool. RNA-sequencing, ultrastructural analysis, and *in vitro* progenitor assays revealed that hepatocyte-derived progenitors were distinct from their biliary-derived counterparts. *In vivo* lineage tracing and serial transplantation assays showed that hepatocyte-derived proliferative ducts retained a memory of their origin and differentiated back into hepatocytes upon cessation of injury. Similarly, human hepatocytes in chimeric mice also gave rise to biliary progenitors *in vivo*. We conclude that human and mouse hepatocytes can undergo reversible ductal metaplasia in response to injury, expand as ducts and subsequently contribute to restoration of the hepatocyte mass.

*Corresponding author: Branden D. Tarlow 3181 S.W. Sam Jackson Park Road Mail code: L321 Portland, Oregon 97239 Phone: 503-621-8136 tarlowb@ohsu.edu.

Keywords

hepatocyte; liver progenitor cell; metaplasia; hepatic differentiation; lineage tracing; mouse; human

Introduction

Liver stem/progenitor cells, or hepatic oval cells, appear and undergo a massive expansion in chronic liver damage. In human disease, the extent of biliary-like progenitor proliferation emanating from the portal triads consistently correlates with the degree of clinical impairment (Lowes et al., 1999; Sancho-Bru et al., 2012). Experimental injury models in rodents designed to model this biliary progenitor proliferation have demonstrated that duct-like "oval cells" can differentiate into both hepatocytes and bile ducts (Evarts et al., 1987; Wang et al., 2003; Yovchev et al., 2008). This finding suggested that the progenitor compartment represents a clinically important cell population that could be pharmacologically manipulated to improve liver function in advanced liver disease where mortality is high and few treatment options currently exist.

A long-standing debate in the field has centered on whether progenitors are derived from biliary-like stem cells that acquire hepatocyte functions or from hepatocytes that lose hepatocyte functions(Farber, 1956; Michalopoulos, 2014; Sell, 1990). Recently, we showed that clonally traced biliary-derived Sox9+ proliferative ducts insignificantly contributed to regeneration of the hepatocyte pool in several classic mouse oval cell injury models(Tarlow et al., 2014). Using increasingly sophisticated lineage tracing tools several other groups have also demonstrated a very limited ability of non-hepatocytes progenitors to contribute to mouse liver regeneration in homeostasis and oval cell injuries (Español-Suñer et al., 2012; Yanger et al., 2014; Schaub et al., 2014).

On the contrary, good evidence now exists that hepatocytes can "transdifferentiate" into ductal biliary epithelial cells in certain injury models(Michalopoulos et al., 2005; Sekiya and Suzuki, 2014; Tanimizu et al., 2014; Yanger et al., 2013) and/or by forced genetic modulation of the developmentally important Notch (Jeliazkova et al., 2013; Yanger et al., 2013) and Hippo pathways(Yimlamai et al., 2014). In the context of cancer, multiple groups have shown that hepatocytes can be transformed into a biliary-cell-like tumor, cholangiocarcinoma, previously thought to originate exclusively from cholangiocytes(Fan et al., 2012; Sekiya and Suzuki, 2012).

Nevertheless, it remains unclear whether hepatocyte-to-duct conversion is reversible or how this process may contribute to liver regeneration. The observation that "dedifferentiated" or "mesenchymal" hepatocytes are primed to reacquire hepatic functions *in vitro* (Chen et al., 2012; Dunn et al., 1989; Santangelo et al., 2011; Tanimizu et al., 2014) raised the question whether hepatocyte-derived progenitors could differentiate back to hepatocytes *in vivo*. Here we characterized hepatocyte-derived progenitors cells in a mouse model of oval cell activation. We utilized hepatocytechimeric mice to test the hypothesis that hepatocyte-to-ductal metaplasia is a reversible process. Our results indicate that both human and mouse hepatocytes undergo metaplasia to a distinctive progenitor state that can be reversed

following recovery, and therefore, may represent a physiologically important pool of hepatocyte precursors in chronic liver injury.

Results

Hepatocytes contribute to the oval cell response after extended injury

To specifically track the fate of mature hepatocytes in liver injury, we generated mice with chimeric livers by transplanting ROSA-mTmG hepatocytes into $Fah^{-/-}$ mice (Fig. 1a). After 10 weeks of repopulation the hepatocyte compartment, but not other cell types, were replaced by donor mTomato+ cells in agreement with previous detailed analyses in our lab (Overturf et al., 1999; Overturf et al., 1997; Tarlow et al., 2014).

Next, we induced a prototypical oval cell injury(Preisegger et al., 1999) by feeding mice a 0.1% 3,5-diethoxycarbonyl-1,4-dihydrocollidine (DDC) diet (Dorrell et al., 2011; Español-Suñer et al., 2012; Huch et al., 2013; Rodrigo-Torres et al., 2014; Yanger et al., 2013). As expected from previous work, 2-weeks of DDC injury induced host-derived OPN+ Krt19+ ductal proliferation in chimeric mice (Fig. 1b).

Following 6-weeks of DDC injury, however, cords of donor hepatocyte-derived mTomato+ cells were prominently observed in the periportal region and co-localized with biliary ductal markers OPN (Fig. 1), SOX9, and A6 (Fig. S2) in agreement with Yanger et. al(Yanger et al., 2013). OPN$^+$ mTomato$^+$ cells had ductal morphology with oval-shaped nuclei. The induction of OPN in mTomato$^+$ hepatocyte-derived ductal cells corresponded with a downregulation of the hepatocyte-marker FAH(Fig. 1c). Hepatocyte-derived ducts incorporated EdU, thus we called these cells hepatocyte-derived proliferative ducts (hepPDs) (Fig. 1d). Despite the emergence of numerous hepPDs, the majority of ducts nonetheless arose from the host and were termed biliary-derived proliferative ducts (bilPDs). As a second, independent method of marking mature hepatocytes we also administered a low dose of a hepatocyte-specific rAAV8-TTR-Cre to adult ROSA-Confetti reporter mice (Malato et al., 2011; Yanger et al., 2013). The findings after 6-weeks of DDC injury were similar to the chimera-based tracing results (n=3). Single clonally marked hepatocytes delineated by a single color of the reporter transgene expanded to cords of 10-40 cells with biliary morphology, indicating hepatocyte-derived duct-like cells were proliferative (Fig. S2).

Isolation of hepatocyte-derived liver progenitors cells with surface marker MIC1-1C3

To further study hepatocyte-derived proliferative ducts (hepPDs) we adapted a FACS-based assay developed by us (Dorrell et al., 2011). We used the pan-ductal marker MIC1-1C3 to isolate antigenically defined cells based on cell surface phenotype (Fig. 2A).

Hepatocyte chimeric ROSA-mTmG / Fah$^{-/-}$ mice were treated for 1 to 8 weeks with DDC to induce oval cell activation. Livers were dissociated into single cells and MIC1-1C3$^+$ CD45$^-$ CD31$^-$ CD11b$^-$ CD26$^-$ PI$^-$ cells ("MIC1-1C3$^+$ cells") were FACS sorted by mTomato-fluorescence status (Fig 2A). Without injury, less than 0.1% of MIC1-1C3$^+$ cells were mTomato$^+$ (median 0.067% n=4). Visual inspection of FACS-positive cells from uninjured mice confirmed that most mTomato$^+$ ductal cells had small portions of adjacent

membrane-localized fluorescent protein likely from an adjacent hepatocyte (Fig. S1). In contrast, 8.7 - 39.3% of MIC1-1C3^{+} oval cells were mTomato[+] after 4-8 weeks of injury, and thus determined to be of donor hepatocyte origin (n = 14) (Fig. 2B). Hepatocyte-to-ductal cell conversion was rare before 14 days of injury and moderately correlated with the duration of injury (linear regression r^2 = 0.63). Again, our secondary marking strategy using low dose rAAV8-Ttr-Cre followed by DDC injury yielded analogous results when FACS phenotyping was used to detect hepatocyte-to-duct metaplasia (Fig. S2).

To further characterize the different populations of ductal progenitors, FACS isolated cells were fixed and analyzed by light and transmission electron microscopy (Fig. 2C-F). Consistent with historical descriptions of "oval cells", hepPDs were highly similar to bile duct epithelium by H&E or Hoechst 33342 staining. Compared with hepatocytes, hepPDs were significantly smaller in cell diameter (mean 14.6μm ± s.d. 3.2 versus 33.1μm ± 4.1; p <0.0001) and the nucleus represented a greater fraction of total cell area (0.417 ± 0.085 versus 0.138 ± .035 versus; p<0.0001). BilPDs were smaller in diameter compared with hepPDs (11.3μm ± 0.9 versus 14.6 ± 3.2; p<0.0001) and had significantly greater fractional nucleus size (0.489 ± 0.054 versus 0.417±0.085; p<0.001). Rare binucleated hepPDs were observed, however, no binucleated bilPDs were found (not shown).

HepPDs exhibited additional ultrastructual differences including a greater abundance of mitochondria and decreased heterochromatin compared with bilPDs. Lysosomal contents in hepPDs were suggestive of autophagy (arrow) as a potential mechanism for organelle and cytoplasm volume reduction. Glycogen granules were found in mature hepatocytes but were largely absent in hepPDs (Fig. S3).

Hepatocyte-derived MIC1-1C3^{+} cells express progenitor-associated genes

To determine whether the morphological differences between donor-derived hepPDs and host-derived bilPDs corresponded to changes in gene expression, mRNA was extracted from FACS-sorted hepatocytes, host-derived MIC1-1C3^{+} cells, and hepatocyte-derived mTomato[+] MIC1-1C3^{+} cells for global expression analysis. RNA-sequencing indicated that 98.4 – 99.2% of mTomato tags were derived from FACS sorted MIC1-1C3[+] mTomato+ cells, within the expected accuracy of FACS isolation (n=4 paired samples, normalized to reads per million). Genotyping for *Fah* confirmed that FACS-sorting based on the mTomato-phenotype effectively separated genetically distinct host from donor-derived progenitor cells (Fig. S4).

FACS-isolated hepatocyte-derived MIC1-1C3^{+} cells from 5 independent experiments showed a unique gene expression phenotype according to unsupervised clustering (Fig 3B) and principle component analyses (Fig. S4). Hepatocyte-derived ducts were more similar to biliary-derived ducts than the corresponding parental hepatocytes isolated from DDC injured chimeras. Nevertheless, more than 2,010 genes were significantly differentially expressed (>2-fold, q<0.01, RPKM>1 in either group) between the two duct progenitor subtypes. 4,714 genes were differentially expressed between hepPDs and parental hepatocytes.

Next we examined expression of genes previously used as lineage tracing promoters to study ductal liver progenitors in mice, including *Sox9*, *Spp1 (*also called *Opn)*, and *Hnf1b* (Fig. 3c)

(Español-Suñer et al., 2012; Furuyama et al., 2010; Rodrigo-Torres et al., 2014). Expression levels of these genes were highly enriched in both progenitor cell types compared with hepatocyes, but hepPDs and bilPDs did not express significantly different levels of *Sox9* (92.44 ± 15.41 mean RPKM ± s.d. v. 102.56 ± 29.11; FDR q-value = 0.87), *Spp1* (17759.8 ± 1095.5 v. 18618.3 ± 587.6; q = 0.84), or *Hnf1b* (158.9 ± 12.9 v. 176.4 ± 21.4; q = 0.72). Thus, conversion of hepatocytes was associated with increased expression of ductal markers. Notably, not all ductal marker genes were highly induced. *Krt19* and *EpCam* were expressed at intermediate levels in hepPDs. For example, *Krt19* levels in hepPDs were 119-fold higher than in hepatocytes (42.53 ± 23.45 RPKM mean ± s.d., n=5 versus 0.36 ± 0.29; n=3, q< 1e-31) but 15-fold lower compared with bilPDs (657.89 ± 65.25; n=5, q <1e-44). Gene expression differences were validated by qRT-PCR (Fig. S4). Interestingly, FACS-sorted hepatocytes expressed the highest levels of the putative progenitor marker *Lgr5* when compared with either progenitor subtype (5.5 or 13.4-fold higher, q < 8e-15).

Compared to the parental mature hepatocytes from which they derive, hepPDs expressed significantly lower levels of albumin (*Alb*), homogentisic acid dehydrogenase (*Hgd*), *Cyp7a1,* the rate limiting enzyme in bile acid biosynthesis, coagulation factor IX (*F9*), and hepatocyte-nuclear factor 4 (*Hnf4a*). Importantly, expression of a subset of hepatocyte-associated genes in hepPDs was similar to bilPDs (e.g. *Alb, Hgd, Cyp7a1*) whereas others were intermediate between hepatocytes and bilPDs (e.g. *Hnf4a, F9*). The fact that mature hepatocyte genes were expressed at ratios different from hepatocytes themselves argues against hepatocyte contamination as the source of these transcripts.

Hepatocyte-to-ductal transition correlates with induction of mesenchymal genes

Gene set enrichment analysis (GSEA) was performed to identify pathways that were differentially active between cell subpopulations. Although hepPDs expressed many ductal progenitor markers at levels similar to bile duct-derived cells, they also retained patterns of gene expression closely associated with hepatocyte function, albeit at a low levels. Compared with bilPDs, hepPDs showed strong enrichment (FDR q-value < 0.05) of gene sets for hepatocyte functions including fatty acid metabolism, complement and coagulation cascades, drug metabolism & cytochrome P450, and branched amino acid degradation. Thus, hepatocyte-derived progenitors retained basal levels of transcription for genes encoding mature hepatocyte functions.

To understand what pathways were driving the hepPD conversion, we compared hepPDs to the parental hepatocyte population. Gene sets for notch signaling pathway, hedgehog signaling pathway, and the Wnt signaling pathway were significantly induced (q < 0.2). Additional gene sets enriched in hepPDs included axon guidance, melanogenesis, tight junctions, and Tgf-β signaling gene sets (q < 0.25).

178 genes were significantly upregulated in hepPDs in pairwise comparisons with both hepatocytes and bilPDs. This finding again shows that the gene expression signature of hepPDs could not be explained by simple hepatocyte contamination. Notably, the transcription factor *Zeb1*, a master regulator epithelial-to-mesenchymal transition (EMT) (Kalluri and Weinberg, 2009) was overexpressed in hepPDs compared with bilPDs (3.6-fold, q < 9e-36) and hepatocytes (3.3-fold, q < 2e-8). Additional genes in this group

associated with EMT included *Vim* (Alison et al., 1996; Demetris et al., 1996)*, Mst1r, Fzd10* and *c-Kit* (Chen et al., 2012; Fujio et al., 1994; Yovchev et al., 2008; Wang et al., 2003). Hepatocyte-derived ducts also showed enrichment of genes expressed in neuronal-progenitors that were previously identified in human ductular reactions or experimentally induced oval cells, including *Nes* (Gleiberman et al., 2005), Neuronalcadherin (also called *Cdh2*) (Mosnier et al., 2009), and *Ncam1* (Shin et al., 2011; Zhou et al., 2007). *Smo*, an intermediate in the hedgehog pathway proposed to regulate epithelial-mesenchymal transitions in the liver(Michelotti et al., 2013), was highly upregulated in hepPDs compared with hepatocytes (36-fold, $q < 1e-16$) but similar to bilPDs ($q = 0.46$). A complete list of enriched gene sets and differentially expressed genes can be found in the Supplemental Information.

Hepatocyte and bile duct-derived oval cells are functionally distinct in vitro

Given that hepatocyte-derived ducts were distinct from bile ducts with respect to gene expression patterns and ultrastructural features, we hypothesized they were also functionally distinct. After 6 weeks of DDC injury, chimeric livers were dissociated into single cells and seeded into our previously published organoid forming assay for liver progenitor activity(Huch et al., 2013). Organoid formation was robust. Despite the fact that hepPDs expressed *Sox9*, *Hnf1b*, and *Lgr5*, we found that organoids were universally negative for fluorescent protein mTomato (Fig 4A). When FACS sorted MIC1-1C3^{+} cells from injured chimeras were seeded into matrigel (500 – 2000 cells/animal), only mTomato-negative host bile duct-derived cells formed organoids, hollow structures >20 cells that could be passaged multiple times (n=6 animals, 50-200 organoids scored/animal). Interestingly, a third of hepPDs and ~1% host MIC1-1C3^{+} cells seeded into matrigel formed mesenchymal-like structures with fillipodia projections (Fig 4D-E). When cultured cells were exposed to hepatocyte-differentiation medium containing dexamethasone and oncostatin-M, hepPDs showed an enhanced ability to upregulate albumin mRNA (Fig 4F) compared with Rspo-1 containing expansion medium. The ability of hepatocyte-derived progenitors to reactivate hepatocyte gene expression *in vitro* is in agreement with a recent publication(Tanimizu et al., 2014).

To confirm that the fluorescent reporter protein was not preventing organoid formation, we switched the reporter to the host by generating Fah^{−/−} ROSA-mTmG mice. We then transplanted these mice with unmarked wild-type hepatocytes. After 6 weeks DDC injury, >10% of MIC1-1C3^{+} cells were hepatocyte-derived by FACS (n=2, Fig. S5). Only host-derived mTomato[+] bilPDs formed organoids, and donor-derived hepPDs cells (MIC1-1C3[+] mTomato[−]) accounted for nearly all cells with mesenchymal filipodia. This finding also provides an additional indication that organoid-forming bile duct progenitor cells did not contribute to repopulation of the Fah^{−/−} liver in the chimerization process(Overturf et al., 1997; 1996; Tarlow et al., 2014). Given that hepPDs expressed a partial-EMT signature and basal levels of hepatocyte-associated genes, we hypothesized that the conversion could be reversed through a mesenchymal-toepithelial transition (MET) (Bin Li et al., 2011; Yovchev et al., 2008).

Sox9+ hepatocyte-derived progenitor cells revert back to hepatocytes in vivo after injury subsides

Continuous DDC injury induced the conversion of some hepatocytes to a highly ductal phenotype. We therefore wondered whether this fate conversion was highly stable as previously suggested(Yanger et al., 2013) or whether the cells retained the ability to revert to their cell of origin upon cessation of the injury. To ask this question, we performed lineage tracing with a tamoxifen-inducible Sox9 reporter. Our RNA-seq expression data (Fig 3) indicated that *Sox9* was expressed at high levels in hepPDs; therefore, we reasoned that a Sox9-CreERT2 allele could be used to specifically track the fate of hepatocyte-derived progenitor cells during an injury recovery period.

Chimeric mice were generated by transplanting gravity-purified Sox9-CreERT2 ROSA-mTmG hepatocytes into Fah$^{-/-}$ recipient mice. We allowed 8-10 weeks for repopulation. Next, we induced oval cell injury in chimeric mice by feeding 0.1% DDC. After 4 weeks a low-dose pulse of tamoxifen (15mg/kg) was given to induce recombination in Sox9+ hepatocyte-derived cells, converting their baseline red color to green. DDC was continued for two additional weeks to allow tamoxifen to wash out and residual mTomato protein to degrade in recombined cells. At the end of the DDC injury 1/3 partial hepatectomy was performed to measure the post-injury frequency of hepatocyte-derived duct cells. Following hepatectomy, animals were placed on a regular diet to allow healing and *in vivo* tracing of hepatocyte-derived liver progenitors in a 4-week recovery period (Fig 5A). Thus, we were able to monitor the phenotype of Sox9- CreERT2 marked hepatocyte derived progenitor cells within *the same* animals before and after injury recovery.

At the peak of injury, the majority of Sox9-marked cells expressed the classic oval cell marker A6 and were arranged in ductal cords (Fig. 5B). At this injury baseline, only a small percentage (6.6%, range 3.5% to 10.5%, n = 4) of Sox9-CreERT2 marked cells co-expressed the hepatocyte-marker FAH (Fig. 5C, D). No tamoxifen-independent recombination was observed (Fig. S6F). Importantly, the frequency of Sox9-marked hepatocytes was markedly increased after a 4 week recovery period in all animals tested (Fig. 5E,F). These cells had hepatocyte morphology and were positive for hepatocyte markers HNF4α and MUP (Fig. S6). The average increase was ~5-fold from the immediate post-injury benchmark: 33.5% (range 22.9% to 38.96%; n=4, paired t-test p = 0.0067, Fig. 5G). This notable shift in the ratio of ductal progenitors:hepatocytes strongly suggested that a significant fraction of hepPDs had redifferentiated back into hepatocytes once the injury subsided. It is worth noting that many hepatocyte-derived ducts had not reactivated the hepatocyte program at the 4-week recovery time point. This may be explained by the fact that signs of liver damage persist in the DDC model for many weeks after reinstitution of a normal diet (Fig. S6).

Clonal analysis of hepatocyte-derived progenitors in a new microenvironment

To further determine whether hepatocyte-derived ducts could revert to functional hepatocytes in the absence of ongoing injury, we performed serial transplantation of marked cells from chimeric mice treated with DDC for 6 weeks. This experiment differs from the lineage tracing after stopping the DDC injury in that the cells were transferred into a liver not undergoing oval cell injury. In this experiment, donor hepatocytes that had not

undergone ductal metaplasia retained their original mTomato red color, whereas cells that transdifferentiated were marked mGFP because of their Sox9 expression. The two populations competed with each other for engraftment and repopulation of a secondary host.

We used low-speed gravity centrifugation to enrich ductal cells for transplantation. Before transplantation 6.3% of ROSA-mTmG cells were mGFP+ (22/333 in 5 random fields, Fig 6B). Over 90% of these had a highly ductal phenotype and did not express mature hepatocyte markers. 2 million total cells were then transplanted into $Fah^{-/-}$ recipient mice and harvested after 5 weeks for analysis (Fig. C). We found that mGFP marked donor cells were nearly as efficient as mTomato marked hepatocytes at engrafting in a new microenvironment: 2.3 – 4.1% of grafts were mGFP+ compared with 6.3% prior to transplant. Importantly, over 60% of the engrafted clones from green marked cells were clearly hepatocytic (range 62% to 81%). They were FAH+, had hepatocyte morphology in terms of size and cell shape, were MUP positive (Fig. S6), and most importantly formed repopulation nodules in the $Fah^{-/-}$ liver (Fig 6D,E). Cells from a DDC treated Sox9-CreERT2 chimera that was not given tamoxifen were transplanted into $Fah^{-/-}$ mice as a control. No green nodules formed in the host, indicating that the hepatocytes were not marked by Sox9-CreERT2 activation in the process of transplantation (0/627 and 0/777 hepatocyte nodules, n=2 mice, not shown). Together, these experiments show that a large fraction of hepPDs converted back to the hepatocyte-fate despite their highly ductal phenotype and gene expression profile. This is in contrast to normal ductal progenitors that lack the ability to produce hepatocytes unless they are expanded and manipulated *in vitro* prior to transplantation (Huch et al 2013).

Human hepatocytes morph into oval cells following sustained injury

Finally, we asked whether the hepatocyte-ductal metaplasia mechanism might be conserved in human hepatocytes. To test the potential of human hepatocytes to undergo ductal metaplasia *in vivo*, we humanized the hepatocyte compartment of $Fah^{-/-}$ $Rag2^{-/-}$ $Il2r\gamma^{-/-}$ (FRG) triple knockout mice by human hepatocyte transplantation(Azuma et al., 2007). Moderately-humanized (>1500ug/mL human serum albumin (HSA)=~30% repopulation) or highly humanized (>4500ug/mL HSA =~90%) FRG mice were administered 0.1% DDC diet for several weeks. The diet was well tolerated and produced hepatomegaly, dramatic darkening of the liver, and ductal proliferation. In 3/6 mice treated with DDC human hepatocytes expressed *EpCAM* and morphed into duct-like cords with poorly defined lumen, oval-shaped nuclei, and scant cytoplasm (Fig. 7B). As a control for antibody specificity, EpCAM+ ductal cords were observed in cirrhotic human liver but not in humanized mice maintained on NTBC or DDC injured mouse hepatocyte chimeras (Fig. S7). EpCAM+ cells co-expressed low levels of FAH, confirming their donor origin. FAH^{low} ductal cords were often adjacent to or intertwined with mouse ductal proliferations with poorly defined lumen(Fig. S7).

Next, whole chimeric livers were homogenized to assess levels of human specific mRNAs. Human *KRT19* mRNA was detected in human liver surgical biopsies but not mouse liver control samples by qRT-PCR (Fig. 7C,D). No humanized animals maintained on normal chow expressed *KRT19* mRNA (n = 0/11) or showed evidence of human KRT19+ cells (Fig.

S7). In contrast, robust induction of *KRT19* was observed in 3 of 6 chimeric mice treated with DDC. *KRT19*^{+} chimeric animals represented 3 different human hepatocyte donors. *KRT19* levels, normalized to human *LAMIN A/C*, ranged from 9-to-285-times lower than normal human liver.

Finally, we wished to determine whether DDC oval cell injury would induce the expression of a range of human bile duct genes in human hepatocytes. We performed RNA-seq on whole liver homogenates and used a custom transcriptome-based index (see Methods) to achieve highly species-specific gene alignment of tags (0.01% - 0.2% erroneous assignment with known single species controls) (Fig. 7E). Compared with humanized mice on normal chow, DDC-fed chimeric mice had increases in multiple bile duct associated genes, including *SPP1*, *SOX9*, *KRT7* (p<0.001); *CD44* (p<0.01); and *VIM* (p<0.05) (Fig. 7F). Together, these data are consistent with the direct conversion of human hepatocytes into biliary-like proliferative ductal cells in chronic liver injury.

Discussion

Until recently, the adult mouse liver was thought to harbor facultative stem cells residing in the biliary duct system and capable of producing both ducts and hepatocytes(Fausto, 2004; Duncan et al., 2009; Huch et al., 2013; Miyajima et al., 2014). Recent work, however, has challenged this traditional view and shown that biliary progenitors are inefficient at producing hepatocytes *in vivo* and do not contribute significantly to the restoration of hepatocyte mass during chronic damage(Tarlow et al., 2014; Yanger et al., 2014). Our data herein provide an alternative and novel model explaining the existence of bipotential oval cells in chronic hepatic injury. We show that conversion of mature hepatocytes into biliary-like progenitor cells is a reversible process. These hepatocyte-derived proliferative ducts display the properties previously ascribed to classic oval cells. They proliferate as ducts in the periportal region of the hepatic lobule and can also produce hepatocyte progeny. Our serial transplantation experiments indicate that hepatocyte-derived progenitors give rise to hepatocytes at a much higher efficiency (>60%) than clonogenic progenitors derived from biliary system (<1%)(Huch et al., 2013).

Our data confirm that mature hepatocytes possess significant phenotypic plasticity and reinforce previous studies(Michalopoulos et al., 2005; Yanger et al., 2013; Yimlamai et al., 2014). Our new observations that hepPDs are distinct from bilPDs based on genome-wide expression profiling, electron microscopy, and functional characterization provides a more complete understanding of their unique properties. Interestingly, quantitative RNA-sequencing indicated that hepatocyte-derived progenitor cells express 119-fold higher levels of *Krt19* than hepatocytes but 15-fold lower levels than bile ducts. This intermediate level of expression could be interpreted either as KRT19^{−} (Malato et al., 2011) or KRT19^{+} (Sekiya and Suzuki, 2014; Yanger et al., 2013) depending on the technical parameters of the immunohistochemistry assay. Our results therefore resolve an apparent contradiction between these previous reports.

Despite the equal expression of "bile duct markers" (ie MIC1-1C3, Sox9, Hnf1b, etc) and similar morphology by light microscopy, hepPDs and bilPDs were derived from different

lineages and were functionally distinct. For these reasons, we propose the general term "metaplasia" is more appropriate than transdifferentiation to describe the plasticity of hepatocytes in liver injury models. Transdifferentiation is a specific type of metaplasia where a cell irreversibly switches from one differentiated cell type into another fully differentiated cell type(Slack, 2009). It appears unlikely that there would be a physiologic requirement for hepatocyte to duct transdifferentiation in oval cell injury. The proliferation of host ducts is robust in DDC induced oval cell injury and all ductal proliferation is of non-hepatocyte origin for the first 2 weeks. Hepatocytes are not needed as a source of new ducts. On the other hand, severe hepatocellular injury has been associated with metaplasia towards numerous endodermal lineages including intestinal crypts (complete with goblet and neuroendocrine cells)(Alison et al., 1996; Elmore and Sirica, 1992) or pancreatic acinar-like cells(Kuo et al., 2009). Additionally, chronic injury-associated metaplasia is widely reported to occur in endoderm-derived epithelial cell types in other organs(Slack, 2009).

We also demonstrated that human hepatocytes possessed similar phenotypic plasticity *in vivo* following liver injury. While classic lineage tracing is not possible in human patients, our study provides the first evidence that normal human hepatocytes can induce ductal progenitor genes during chronic injury *in vivo*. This suggests that hepatocyte-metaplasia may also occur in human cirrhosis and that hepatocytes may be a source of ductular reactions in long-term injury. Our dataset provides a specific gene-expression signature of both human and mouse hepatocyte-derived progenitors that may serve as a resource for future investigations (Supplemental Information). We hypothesize that hepatocyte-derived human progenitors would express EMT-associated genes, intermediate levels of *KRT19*, and exhibit unique characteristics in functional assays.

Hepatocytes were until recently considered a terminally differentiated cell that could replicate in acute hepatectomy but not chronic injuries(Miyajima et al., 2014). More broadly, the concept of terminal differentiation of mature cell types has been challenged by numerous demonstrations that cells can change their phenotype during both development and adulthood(Sánchez Alvarado and Yamanaka, 2014). Cellular plasticity induced by the epithelial-to-mesenchymal transition (EMT) program has been found to generate cells that exhibit stem-like properties, particularly in tissue repair, chronic inflammation, and neoplasia (Kalluri and Weinberg, 2009). The acquisition of mesenchymal features is associated with increased migration, resistance to apoptosis, degradation of the basement membrane, increased production of extracellular matrix, and expression of stem/progenitor markers—all which are associated with oval cell activation in chronic liver injury. In our study, the conversion of mature hepatocytes into biliary-like progenitors is marked by induction of mesenchymal markers *Vim*, *Zeb1*, *Cdh2* as well as stem/progenitor markers like *Sox9*, *c-kit*, *Tnfrsf12a* (also called *Fn14*), and *Cd44*. Various signaling pathways activate and maintain the EMT program including the Wnt/β-catenin and Tgf-β pathways (Kalluri and Weinberg, 2009). Our gene-set analysis identified Wnt and Tgf-β family signaling in addition to Notch(Jeliazkova et al., 2013) and hedgehog(Michelotti et al., 2013) signaling associated with hepatocyte-to-progenitor conversion. These data suggest multiple signaling events are responsible for the direct conversion of mature hepatocytes to progenitor cells and are consistent with an EMT-like process. Although genetic experiments have clearly shown

a role for the Hippo signaling pathway in maintenance of the hepatocyte phenotype(Yimlamai et al., 2014), its significance in oval cell injury induced metaplasia remains uncertain. Further mechanistic studies in well-defined conditions are needed to understand molecular mechanisms underlying the expression of mesenchymal genes.

Hepatocyte-ductal metaplasia observed here follows the same pattern of epithelial-tomesenchymal transition where transitioning cells later revert to their original state through mesenchymal-to-epithelial transition (MET) (Tam and Weinberg, 2013). In fact, fetal liver stem cells downregulate vimentin and other mesenchymal markers as they differentiate into parenchymal epithelial cells(Bin Li et al., 2011). Similarly, oval cells in the classic 2-AAF/ partial hepatectomy model reversibly induce mesenchymal markers including Vimentin and Bmp7(Alison et al., 1996; Yovchev et al., 2008).

It is not currently known whether ductal-metaplasia is an adaptive or maladaptive process. We hypothesize that hepatocyte-ductal-metaplasia is an injury evasion strategy that is facilitated by bile duct proliferation. Metaplasia provides a mechanism to shut down the hepatocyte-gene expression program in order to avoid insults that are specifically toxic to hepatocytes but harm few other cell types (i.e. hepatitis virus, Cyp450-activated toxins, etc). This permits individual cells to improve their fitness. In our "decoy metaplasia" model (see Graphical Abstract), the hepPD pool expands in the presence of a regenerative stimulus. If the injury is transient and eventually regresses, these hepPDs can revert back to their original fate: a mature hepatocyte.

Improving the efficiency of progenitor-to-hepatocyte reversion with pharmacologic agents may represent a future strategy to improve hepatic function and outcomes in decompensated liver failure. Additionally, the propagation of hepatocyte-derived progenitor cells *in vitro* may provide an opportunity for autologous cell therapy in regenerative medicine applications. We speculate that a better understanding of the epigenetic mechanisms of "decoy metaplasia" in injury models may provide an opportunity for targeted therapies to provide a bridge to liver transplantation.

Materials and methods

Full details are provided in the **Extended Experimental Procedures**

Mouse strains, chimera generation, and diet

Sox9-CreERT2 (gift from Dr. Maike Sander), $Fah^{-/-}$, and ROSA-mTomato/mGFP ("ROSA-mTmG") reporter mice maintained on a C57bl/6 background. To generate chimeras, donor $Fah^{+/+}$ hepatocytes were gravity purified ($3 \times 1' \times 50 \times g$) and 4×10^5 liver hepatocytes were injected into the spleen of Fah$^{-/-}$ mice as previously described. (Tarlow et al., 2014). Fah$^{-/-}$ animals were weaned from NTBC on the day of cell transplantation and maintained on water thereafter. Liver injury was induced by feeding 0.1% DDC (3,5-diethoxycarbonyl-1,4-dihydrocollidine, TCI America, Portland, OR) in Purina 5015 chow (TD.120495, Harlan Tekland). To isolate ductal cells from DDC-treated livers, post-perfusion digestion was performed with Collagenase II and TrypLE(Dorrell et al., 2011). Cells that did not pellet after $2 \times 1' \times 50g$ were considered the non-parenchymal fraction and

used for FACS and serial transplantation experiments. Tamoxifen was resuspended in sesame oil (30mg/mL) and given by intraperitoneal injection to Sox9-CreERT2 ROSA-mTmG chimeric mice.

Modifications for serial transplantation experiments enrichment of nonparenchymal cells by gravity centrifugation ($2 \times 1' \times 50g$, non-pelleting cells). Recipient mice were given adenoviral urokinase-plasminogen activator (Ad-uPA) (5×10^7 pfu/g body weight) to improve trapping of small diameter donor cells. Virus was given 48 hours prior to cell transplantation by retroorbital or tail vein injection under isofluorane anesthesia. Animals were cycled back on NTBC once during a 5-week selection period.

Cryopreserved human hepatocytes (Life Technologies, Inc) were thawed and washed. The hepatoyctes were centrifuged at $100 \times g$ for 5 minutes at $4°C$ and reconstituted at 10e6 cells/mL. 4e5 live cells were injected to the spleen of recipient $Fah^{-/-} Rag2^{-/-} Il2rg^{-/-}$ (FRG-NOD) mice (Yecuris, Inc). FRG-NOD mice received (Ad-uPA) 48 hours prior to transplantation. Post-transplant, a standard NTBC cycling protocol was followed to promote human hepatocyte selection. Sulfamethoxazole-trimethoprim was included in the drinking water in a subset of animals as an antimicrobial prophylactic. All procedures and protocols with vertebrate animals were approved by the OHSU IACUC.

FACS analysis

Liver NPCs were isolated by a multi-step collagenase (type IV, type D) perfusion and labeled with antibodies as previously described (Dorrell et al., 2011). Cells were sorted on an inFlux cytometer (BD Biosciences) equipped with 405, 488, 561 and 640nm excitation lasers. Double positive events were visually inspected to exclude the possibility of two cells stuck together.

Cell culture

Crude non-parenchymal cell fractions were enriched by gravity or FACS. 500 to 20,000 cells were seeded into 60μL matrigel droplets. Growth media included B27 supplement, N2 supplement, Wnt3a, Egf, Hgf, and Rspo1-Fc; differentiation media included dexamethasone and OSM as previously described (Huch et al., 2013).

Gene expression analysis

FACS sorted mouse cells were lysed in Trizol (Life Technologies) and treated with chloroform. Whole human-mouse chimeric livers were directly homogenized without cell fractionation. The aqueous layer was precipitated with ethanol and applied to silica columns for purification and DNAse digestion (Qiagen RNAeasy Mini or Micro). The organic layer was saved for later DNA isolation. Samples meeting quality control thresholds (>20,000 cells, RNA integrity RIN >8.5, total RNA > 75ng) were prepared into barcoded libraries with the Truseq RNA Sample Prep Kit v2 according to the manufacturer's instructions (Illumina, Inc). Samples were sequenced on a HiSeq2000 (3-4 samples per lane, single end 50bp reads) to yield an average of 33.1 million exon-mapped tags per FACS sorted sample. RNAseq fastq files and analyzed data are available from the NCBI (http://www.ncbi.nlm.nih.gov/geo/) under accession numbers GSE55552 and GSE58679.

Immunohistochemistry & microscopy

For transmission electron microscopy, 5×10^4 FACS sorted cells were pelleted and fixed in 3% gluteraldehyde at room temperature immediately after isolation. Cell pellets were osmicated, dehydrated, and embedded in araldite resin. Thin sections were stained with uranyl acetate and lead citrate. Then cells were processed with high- pressure freezing and imaged. FACS isolated cells were fixed for 15 minutes in 4% paraformaldehyde (PFA) and cytospun onto charged slides (5' $\times$ 200g). Cells subsequently processed for immunohistochemistry or hemotoxylin and eosin staining. Liver tissues were fixed in 4% paraformaldehyde and cryopreserved in 30% sucrose prior to freezing in OCT tissue blocks. When possible, tissues were fixed with PFA perfusion into the portal vein. Otherwise resected tissues were submerged directly in PFA and fixed for >4 hours. See **Extended Experimental Procedures** for antibody information and immunohistochemistry.

Image analysis

Images were quantified and analyzed using ImageJ software (www.fiji.sc). For serial transplantation experiments fluorescent images were capture immediately before transplantation on a hemocytometer. For analysis of engrafted livers nodule diameter was measured in tiled sections. To correct for differential probability of identifying large spherical nodules in 2-dimension sections, a correction factor was applied as previously described (Wang et al., 2002).

Supplementary Material

Refer to Web version on PubMed Central for supplementary material.

Acknowledgments

Abbreviations

AAV8	adeno-associated virus serotype 8
Ad-uPA	adenoviral urokinase plasminogen activator
bilPD	biliary-derived proliferative duct
hepPD	hepatocyte-derived proliferative duct
DDC	3,5-diethoxycarbonyl-1,4-dihydrocollidine
EMT	epithelial-to mesenchymal transition
EdU	5-ethynyl-2'-deoxyuridine
FACS	fluorescence activated cell sorting

FRG	Fah$^{-/-}$ Rag2$^{-/-}$ Il2r$\gamma^{-/-}$
GSEA	Gene set enrichment analysis
H&E	hematoxylin and eosin
HSA	human serum albumin
MET	mesenchymal-to-epithelial transition
mTmG	membranous-Tomato/membranous-GFP dual fluorescent reporter gene
MUP	major urinary protein
NTBC	2-(2-nitro-4-3 trifluoro-methylbenzoyl)-1,3- cyclohexanedione
OPN	Osteopontin (same as secreted phosphoprotein 1 or Spp1)
PI	Propidium iodide
RPKM	Reads Per Kilobase per Million
Sox9	SRY (Sex- Determining Region Y)-Box 9

References

Alison MR, Golding M, Sarraf CE, Edwards RJ, Lalani EN. Liver damage in the rat induces hepatocyte stem cells from biliary epithelial cells. Ygast. 1996; 110:1182–1190.

Azuma H, Paulk N, Ranade A, Dorrell C, Al-Dhalimy M, Ellis E, Strom S, Kay MA, Finegold M, Grompe M. Robust expansion of human hepatocytes in Fah–/–/Rag2–/–/Il2rg–/– mice. Nat Biotechnol. 2007; 25:903–910. [PubMed: 17664939]

Li, Bin; Zheng, Y-W.; Sano, Y.; Taniguchi, H. Evidence for Mesenchymal–Epithelial Transition Associated with Mouse Hepatic Stem Cell Differentiation. PLoS ONE. 2011; 6:e17092. [PubMed: 21347296]

Chen Y, Wong PP, Sjeklocha L, Steer CJ, Sahin MB. Mature hepatocytes exhibit unexpected plasticity by direct dedifferentiation into liver progenitor cells in culture. Hepatology. 2012; 55:563–574. [PubMed: 21953633]

Demetris AJ, Seaberg EC, Wennerberg A, Ionellie J, Michalopoulos GK. Ductular reaction after submassive necrosis in humans. Special emphasis on analysis of ductular hepatocytes. Am J Pathol. 1996; 149:439–448. [PubMed: 8701983]

Dorrell C, Erker L, Schug J, Kopp JL, Canaday PS, Fox AJ, Smirnova O, Duncan AW, Finegold MJ, Sander M, et al. Prospective isolation of a bipotential clonogenic liver progenitor cell in adult mice. Genes Dev. 2011; 25:1193–1203. [PubMed: 21632826]

Duncan AW, Dorrell C, Grompe M. Stem cells and liver regeneration. Gastroenterology. 2009; 137:466–481. [PubMed: 19470389]

Dunn JC, Yarmush ML, Koebe HG, Tompkins RG. Hepatocyte function and extracellular matrix geometry: long-term culture in a sandwich configuration. Faseb J. 1989; 3:174–177. [PubMed: 2914628]

Elmore LW, Sirica AE. Sequential appearance of intestinal mucosal cell types in the right and caudate liver lobes of furan-treated rats. Hepatology. 1992; 16:1220–1226. [PubMed: 1427660]

Español-Suñer R, Carpentier R, Van Hul N, Legry V, Achouri Y, Cordi S, Jacquemin P, Lemaigre FP, Leclercq IA. Liver Progenitor Cells Yield Functional Hepatocytes in Response to Chronic Liver Injury in Mice. Gastroenterology. 2012; 143:1564–1575. e1567. [PubMed: 22922013]

Evarts RP, Nagy P, Marsden E, Thorgeirsson SS. A precursor-product relationship exists between oval cells and hepatocytes in rat liver. Carcinogenesis. 1987; 8:1737–1740. [PubMed: 3664968]

Fan B, Malato Y, Calvisi DF, Naqvi S, Razumilava N, Ribback S, Gores GJ, Dombrowski F, Evert M, Chen X, et al. Cholangiocarcinomas can originate from hepatocytes in mice. J Clin Invest. 2012; 122:2911–2915. [PubMed: 22797301]

Farber E. Similarities in the sequence of early histological changes induced in the liver of the rat by ethionine, 2-acetylamino-fluorene, and 3′-methyl-4-dimethylaminoazobenzene. Cancer Res. 1956; 16:142–148. [PubMed: 13293655]

Fausto N. Liver regeneration and repair: hepatocytes, progenitor cells, and stem cells. Hepatology. 2004; 39:1477–1487. [PubMed: 15185286]

Fujio K, Evarts RP, Hu Z, Marsden ER, Thorgeirsson SS. Expression of stem cell factor and its receptor, c-kit, during liver regeneration from putative stem cells in adult rat. Lab Invest. 1994; 70:511–516. [PubMed: 7513770]

Furuyama K, Kawaguchi Y, Akiyama H, Horiguchi M, Kodama S, Kuhara T, Hosokawa S, Elbahrawy A, Soeda T, Koizumi M, et al. Continuous cell supply from a Sox9-expressing progenitor zone in adult liver, exocrine pancreas and intestine. Nat Genet. 2010; 43:34–41. [PubMed: 21113154]

Gleiberman AS, Encinas JM, Mignone JL, Michurina T, Rosenfeld MG, Enikolopov G. Expression of nestin-green fluorescent protein transgene marks oval cells in the adult liver. Dev. Dyn. 2005; 234:413–421. [PubMed: 16127706]

Huch M, Dorrell C, Boj SF, van Es JH, Li VSW, van de Wetering M, Sato T, Hamer K, Sasaki N, Finegold MJ, et al. In vitro expansion of single Lgr5(+) liver stem cells induced by Wnt-driven regeneration. Nature. 2013; 494:247–250. [PubMed: 23354049]

Jeliazkova P, Jörs S, Lee M, Zimber-Strobl U, Ferrer J, Schmid RM, Siveke JT, Geisler F. Canonical Notch2 signaling determines biliary cell fates of embryonic hepatoblasts and adult hepatocytes independent of Hes1. Hepatology. 2013; 57:2469–2479. [PubMed: 23315998]

Kalluri R, Weinberg RA. The basics of epithelial-mesenchymal transition. J Clin Invest. 2009; 119:1420–1428. [PubMed: 19487818]

Kuo F-Y, Swanson PE, Yeh MM. Pancreatic acinar tissue in liver explants: a morphologic and immunohistochemical study. The American Journal of Surgical Pathology. 2009; 33:66–71. [PubMed: 18987542]

Lowes KN, Brennan BA, Yeoh GC, Olynyk JK. Oval Cell Numbers in Human Chronic Liver Diseases Are Directly Related to Disease Severity. American Journal of Pathology. 1999; 154:537–541. [PubMed: 10027411]

Malato Y, Naqvi S, Schürmann N, Ng R, Wang B, Zape J, Kay MA, Grimm D, Willenbring H. Fate tracing of mature hepatocytes in mouse liver homeostasis and regeneration. J Clin Invest. 2011; 121:4850–4860. [PubMed: 22105172]

Michalopoulos GK. The liver is a peculiar organ when it comes to stem cells. Am J Pathol. 2014; 184:1263–1267. [PubMed: 24681248]

Michalopoulos GK, Barua L, Bowen WC. Transdifferentiation of rat hepatocytes into biliary cells after bile duct ligation and toxic biliary injury. Hepatology. 2005; 41:535–544. [PubMed: 15726663]

Michelotti GA, Xie G, Swiderska M, Choi SS, Karaca G, Krüger L, Premont R, Yang L, Syn W-K, Metzger D, et al. Smoothened is a master regulator of adult liver repair. J Clin Invest. 2013

Miyajima A, Tanaka M, Itoh T. Stem/progenitor cells in liver development, homeostasis, regeneration, and reprogramming. Cell Stem Cell. 2014; 14:561–574. [PubMed: 24792114]

Mosnier J-F, Kandel C, Cazals-Hatem D, Bou-Hanna C, Gournay J, Jarry A, Laboisse CL. N-cadherin serves as diagnostic biomarker in intrahepatic and perihilar cholangiocarcinomas. Mod. Pathol. 2009; 22:182–190. [PubMed: 18622386]

Overturf K, Al-Dhalimy M, Finegold M, Grompe M. The repopulation potential of hepatocyte populations differing in size and prior mitotic expansion. Am J Pathol. 1999; 155:2135–2143. [PubMed: 10595942]

Overturf K, Al-Dhalimy M, Ou CN, Finegold M, Grompe M. Serial transplantation reveals the stem-cell-like regenerative potential of adult mouse hepatocytes. Am J Pathol. 1997; 151:1273–1280. [PubMed: 9358753]

Overturf K, Al-Dhalimy M, Tanguay R, Brantly M, Ou CN, Finegold M, Grompe M. Hepatocytes corrected by gene therapy are selected in vivo in a murine model of hereditary tyrosinaemia type I. Nat Genet. 1996; 12:266–273. [PubMed: 8589717]

Preisegger KH, Factor VM, Fuchsbichler A, Stumptner C, Denk H, Thorgeirsson SS. Atypical ductular proliferation and its inhibition by transforming growth factor beta1 in the 3,5-diethoxycarbonyl-1,4-dihydrocollidine mouse model for chronic alcoholic liver disease. Lab Invest. 1999; 79:103–109. [PubMed: 10068199]

Rodrigo-Torres D, Affò S, Coll M, Morales-Ibanez O, Millán C, Blaya D, Alvarez-Guaita A, Rentero C, Lozano JJ, Maestro MA, et al. The biliary epithelium gives rise to liver progenitor cells. Hepatology. 2014

Roskams TA, van den Oord JJ, De Vos R, Desmet VJ. Neuroendocrine features of reactive bile ductules in cholestatic liver disease. Am J Pathol. 1990; 137:1019–1025. [PubMed: 1700614]

Sancho-Bru P, Altamirano J, Rodrigo-Torres D, Coll M, Millán C, José Lozano J, Miquel R, Arroyo V, Caballería J, Ginès P, et al. Liver progenitor cell markers correlate with liver damage and predict short-term mortality in patients with alcoholic hepatitis. Hepatology. 2012; 55:1931–1941. [PubMed: 22278680]

Santangelo L, Marchetti A, Cicchini C, Conigliaro A, Conti B, Mancone C, Bonzo JA, Gonzalez FJ, Alonzi T, Amicone L, et al. The stable repression of mesenchymal program is required for hepatocyte identity: a novel role for hepatocyte nuclear factor 4α. Hepatology. 2011; 53:2063–2074. [PubMed: 21384409]

Sánchez Alvarado A, Yamanaka S. Rethinking Differentiation: Stem Cells, Regeneration, and Plasticity. Cell. 2014; 157:110–119. [PubMed: 24679530]

Schaub JR, Malato Y, Gormond C, Willenbring H. Evidence against a stem cell origin of new hepatocytes in a common mouse model of chronic liver injury. Cell Rep. 2014; 8:933–939. [PubMed: 25131204]

Sekiya S, Suzuki A. Intrahepatic cholangiocarcinoma can arise from Notch-mediated conversion of hepatocytes. J Clin Invest. 2012; 122:3914–3918. [PubMed: 23023701]

Sekiya S, Suzuki A. Hepatocytes, Rather than Cholangiocytes, Can Be the Major Source of Primitive Ductules in the Chronically Injured Mouse Liver. Am J Pathol. 2014:1–12.

Sell S. Is there a liver stem cell? Cancer Res. 1990; 50:3811–3815. [PubMed: 1693878]

Shin S, Walton G, Aoki R, Brondell K, Schug J, Fox A, Smirnova O, Dorrell C, Erker L, Chu AS, et al. Foxl1-Cre-marked adult hepatic progenitors have clonogenic and bilineage differentiation potential. Genes Dev. 2011; 25:1185–1192. [PubMed: 21632825]

Slack J. Metaplasia and somatic cell reprogramming. J Pathol. 2009; 217:161–168. [PubMed: 18855879]

Tam WL, Weinberg RA. The epigenetics of epithelial-mesenchymal plasticity in cancer. Nat Med. 2013; 2013; 19:1438–1449. [PubMed: 24202396]

Tanimizu N, Nishikawa Y, Ichinohe N, Akiyama H, Mitaka T. Sry HMG Box Protein 9-positive (Sox9+) Epithelial Cell Adhesion Molecule-negative (EpCAM-) Biphenotypic Cells Derived from Hepatocytes Are Involved in Mouse Liver Regeneration. J. Biol. Chem. 2014; 289:7589–7598. [PubMed: 24482234]

Tarlow BD, Finegold MJ, Grompe M. Clonal tracing of Sox9(+) liver progenitors in mouse oval cell injury. Hepatology. 2014; 60:278–289. [PubMed: 24700457]

Wang X, Foster M, Al-Dhalimy M, Lagasse E, Finegold M, Grompe M. The origin and liver repopulating capacity of murine oval cells. Proc Natl Acad Sci USA 100 Suppl. 2003; 1:11881–11888.

Wang X, Montini E, Al-Dhalimy M, Lagasse E, Finegold M, Grompe M. Kinetics of Liver Repopulation after Bone Marrow Transplantation. Am J Pathol. 2002; 161:565–574. [PubMed: 12163381]

Yanger K, Knigin D, Zong Y, Maggs L, Gu G, Akiyama H, Pikarsky E, Stanger BZ. Adult hepatocytes are generated by self-duplication rather than stem cell differentiation. Cell Stem Cell. 2014; 15:340–349. [PubMed: 25130492]

Yanger K, Zong Y, Maggs LR, Shapira SN, Maddipati R, Aiello NM, Thung SN, Wells RG, Greenbaum LE, Stanger BZ. Robust cellular reprogramming occurs spontaneously during liver regeneration. Genes Dev. 2013; 27:719–724. [PubMed: 23520387]

Yimlamai D, Christodoulou C, Galli GG, yanger K, Pepe-Mooney B, Gurung B, Shrestha K, Cahan P, Stanger BZ, Camargo FD. Hippo pathway activity influences liver cell fate. Cell. 2014; 157:1324–1338. [PubMed: 24906150]

Yovchev MI, Grozdanov PN, Zhou H, Racherla H, Guha C, Dabeva MD. Identification of adult hepatic progenitor cells capable of repopulating injured rat liver. Hepatology. 2008; 47:636–647. [PubMed: 18023068]

Zhou H, Rogler LE, Teperman L, Morgan G, Rogler CE. Identification of hepatocytic and bile ductular cell lineages and candidate stem cells in bipolar ductular reactions in cirrhotic human liver. Hepatology. 2007; 45:716–724. [PubMed: 17326146]
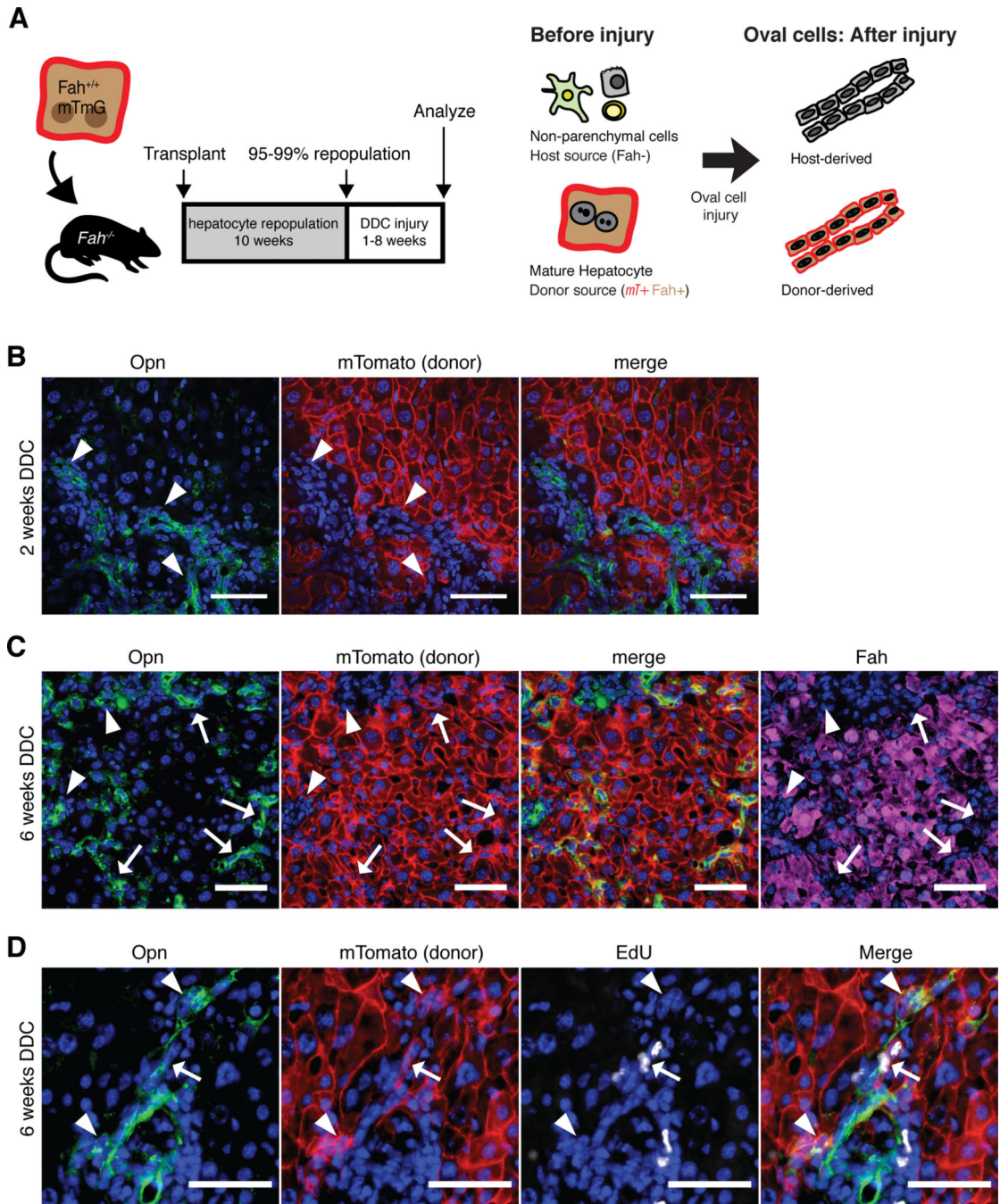
Figure 1. Hepatocyte-derived oval cells appear after extended injury

A) Purified hepatocytes fluorescently marked hepatocytes were transplanted into the spleen of Fah$^{-/-}$ animals. After 10 weeks repopulation, DDC injury was given for 1 to 8 weeks. Since only hepatocytes were marked at baseline, any fluorescent marked ductal cells observed after injury were inferred to be hepatocytes-derived. B) OPN$^+$ ductal proliferation did not colocalize with hepatocyte marker mTomato after 2 weeks injury (arrowhead, bar = 50μm). C) After 6 weeks of injury, a subset of OPN$^+$ ductal cells co- localized with hepatocyte derived mTomato marked cells (arrow), however, the majority of ductal

proliferation was still host-derived (arrowhead). Induction of OPN correlated with the loss of FAH(arrows), bar = 50μm. D) Hepatocyte-derived progenitors (mTomato$^+$ OPN$^+$) incorporated EdU 6 hours after a pulse after 6 weeks of injury.
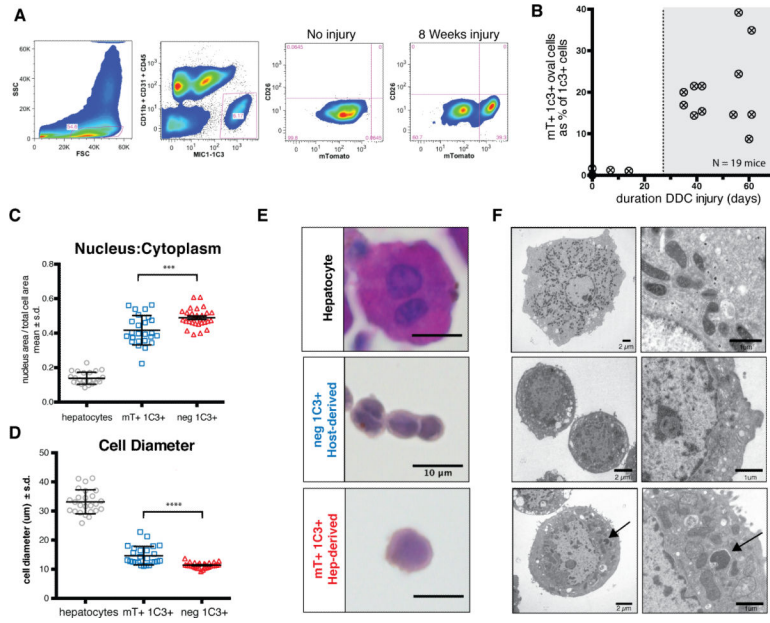
Figure 2. Hepatocyte-derived liver progenitors cells are isolated with MIC1-1C3 antibody
A) Dissociated livers were FACS sorted with gates applied for FSC/SSC (to include ductal cells, as shown), pulse width (not shown), PI− (not shown), and MIC1-1C3+ CD11b− CD31− CD45−. MIC1-1C3+ cell were separated based on mTomato fluorescence (mature hepatocyte origin). Without injury mTomato+ cells were a trace component of MIC1-1C3+ population but increased with injury. B) The percentage of ductal cells derived from mTomato-marked hepatocytes is plotted against the number of days of DDC injury. Hepatocyte-derived MIC1-1C3+ ductal progenitors emerged after approximately 4 weeks injury. C) FACS isolated populations were fixed and nucleus to cytoplasmic ratios and D) cell diameter and were examined for each population (pairwise t-test, p<0.001 ***, p<0.0001****). E) Representative H&E staining (bars = 10μm) and F) transmission electron microscopy from directly isolated cells from each population (bar size indicated). The arrow indicates a membrane bound structure in a lysosome adjacent to mitochondria.
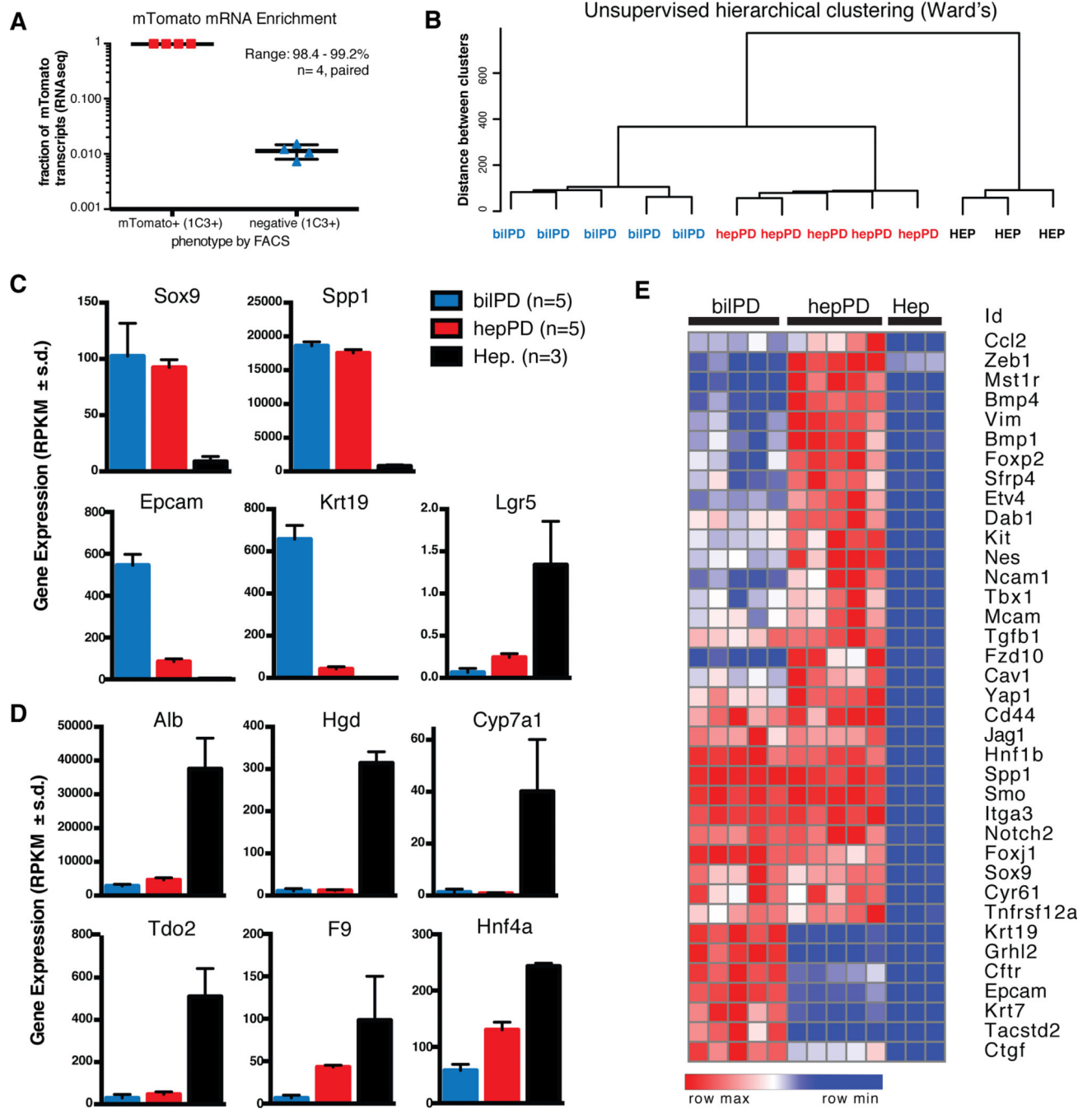
Figure 3. Hepatocyte-derived oval cells are transcriptional distinct from bile ducts

A) FACS separation of MIC1-1C3$^+$ cells based on ROSA-mTomato resulted in 98.4-99.2% enrichment in mTomato$^+$ cells relative to mTomato$^-$ cells (paired analysis, n=4 animals). B) Unsupervised hierarchical clustering (Ward's method) of hepPDs (n=5) bilPDs (n=5), and hepatocytes (n=3). C) Gene expression levels (RPKM) for progenitor associated genes and D) Hepatocyte-associated genes (mean ± s.d.). E) Cluster analysis shows hepPDs express biliary progenitor associated genes and a distinctive mesenchymal signature.
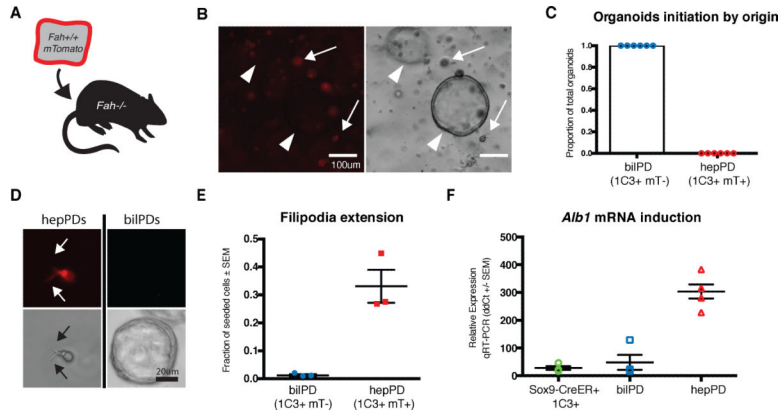
Figure 4. hepPDs are functionally distinct *in vitro*
A) Fah$^{-/-}$ mice were repopulated with Fah$^{+/+}$ Rosa-mTomato$^+$ hepatocytes and injured with DDC. B) Organoids derived from crude non-parenchymal preps from DDC injured chimeric liver were seeded in matrigel for organoid formation. Hepatocyte-derived mTomato$^+$ cells (arrows) did not initiate organoids. All organoids were mTomato (arrowhead). C) MIC1-1C3$^+$ mTomato$^+$ and mTomato- cells were seeded into matrigel for organoid formation. All organoids were host-derived (50-200 counted/animal, n=6 animals). D) hepPDs formed fillipodia (arrows) in matrigel while mTomato$^-$ bilPDs formed spherical organoids. E) Fillipodia formation was quantified as a fraction of seeded cells. F) hepPDs cultured in hepatic differentiation medium induced albumin mRNA with 10.8-fold greater efficiency than bilPDs or MIC1-1C3$^+$ cells from uninjured Sox9-CreERT2 reporter mice (unpaired t-test, p<0.001***).
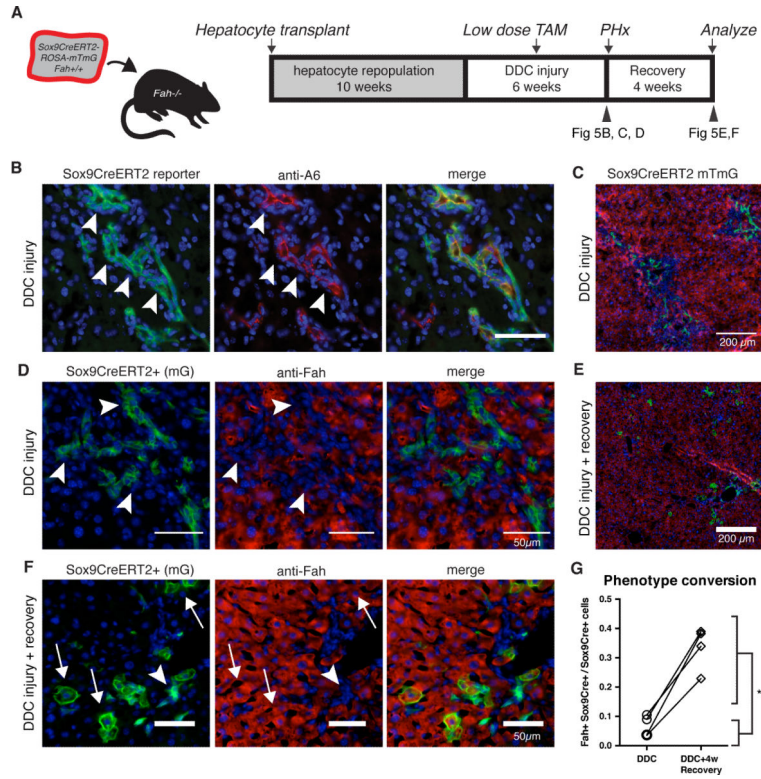
Figure 5. hepPDs revert back to hepatocyctes *in vivo*
A) Fah$^{+/+}$ ROSA-mTmG Sox9-CreERT2 hepatocytes were transplanted into Fah$^{-/-}$ recipients to generate chimeras. DDC injury was given to repopulated chimeras for 4 weeks, a low dose pulse of tamoxifen was given (15mg/kg), and injury was continued for 2 additional weeks. B) Tissue harvested by 1/3 partial hepatectomy showed most Sox9-CreERT2 marked (mGFP+) cells co-localized with A6 antigen (arrowhead). C) Low-power view shows Sox9-marked ductal cells in periportal zone. D) Sox9-CreERT2- marked cells have biliary morphology that do not co-localize with hepatocyte marker FAH. E) Following a 4-week recovery period, mGFP+ hepatocytes localized in the portal area. F) Upon healing Sox9-CreERT2 marked cells assumed hepatocyte morphology co-localized with FAH (arrow). G) Within animal comparison indicated that recovery from DDC injury was associated with a 5-fold increase in marked hepatocytes (6.6% versus 33.5%, $p < 0.01$**, paired t-test, n=4).
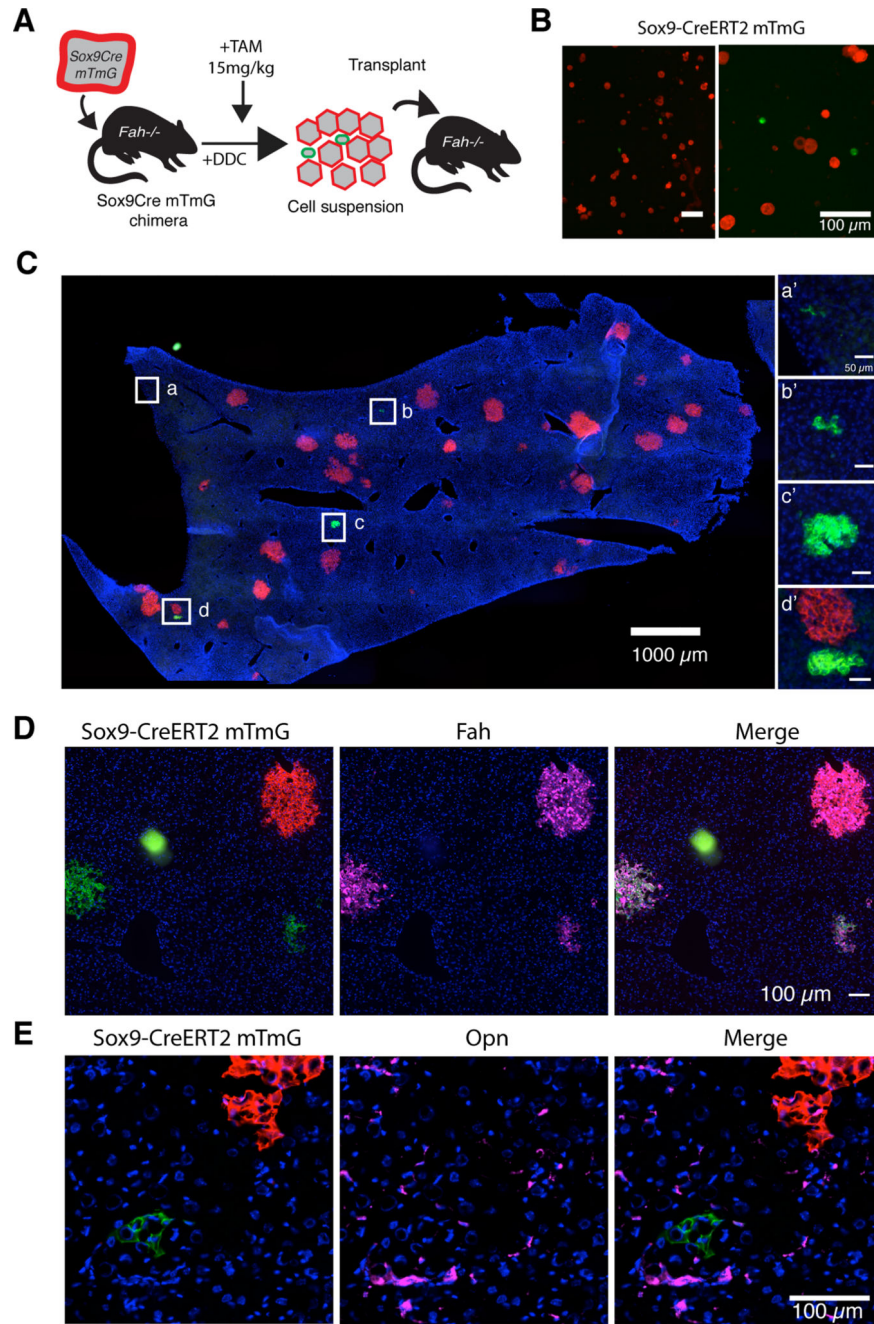
Figure 6. hepPDs differentiate back into hepatocytes upon serial transplantation
A) mGFP+ hepPD and mTomato+ hepatocytes were dissociated as single cells from DDC-injured chimeric mice for intrasplenic transplantation into Fah-/- mice. B) Sox9- CreERT2+ mGFP+ cells were smaller than hepatocytes and represented 6.3% of mTmG cells scored in 5 random fields before transplantation. C) After 5-weeks NTBC cycling, we assessed the rate at which mGFP+ hepPDs contributed to repopulation. mGFP+ clones were smaller than mTomato+ clones D) Hepatocyte-nodules expressed hepatocyte marker FAH but E) not biliary/progenitor marker OPN.
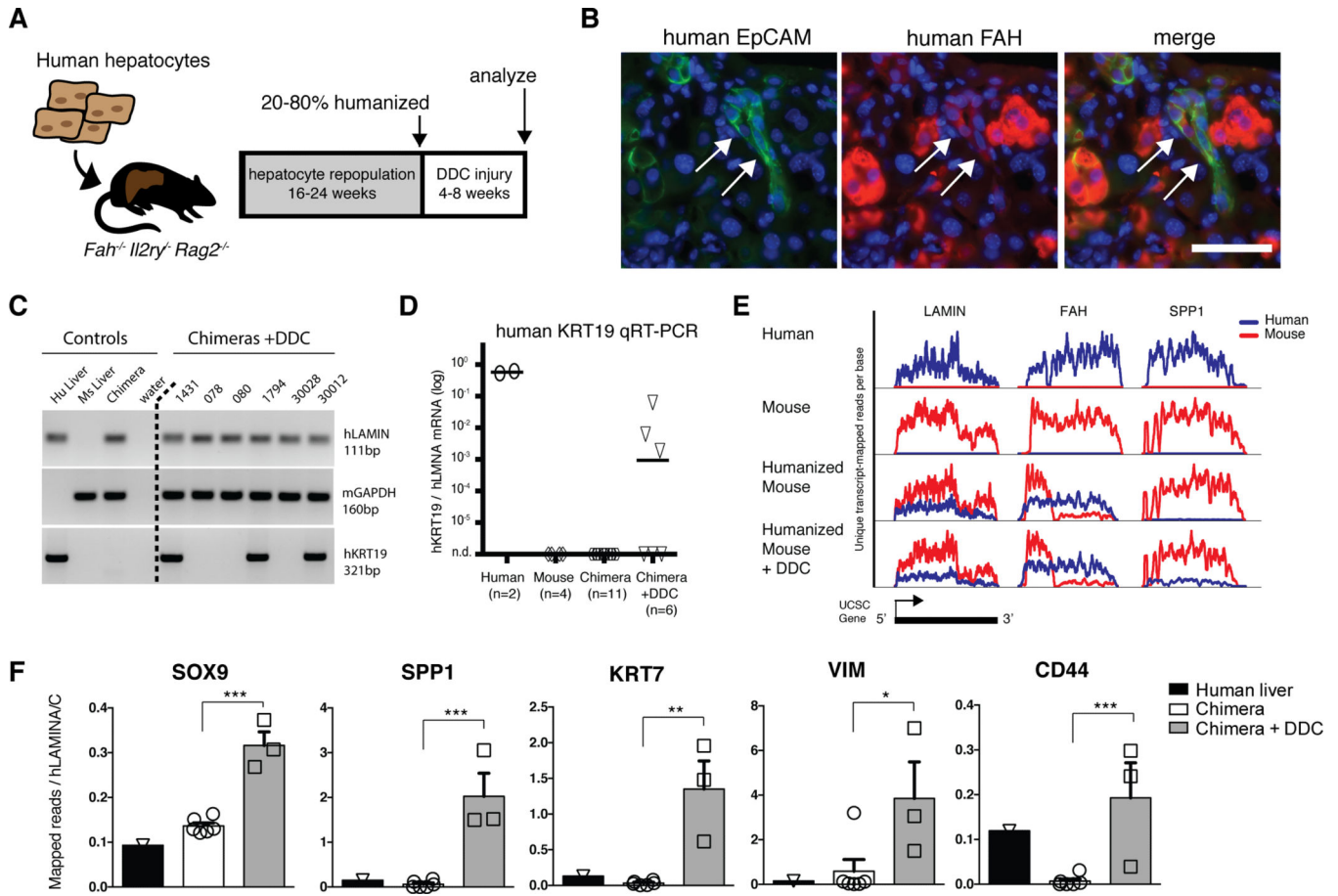
Figure 7. Human hepatocytes are directly converted into biliary-like cells *in vivo*
A) Human hepatocyte were transplanted into FRG mice. After 16-24 weeks repopulation, animals were fed 0.1% DDC for 4-8 weeks. B) After injury, human EpCAM+ FAH^{low} cells with ductal morphology emerged. C) *KRT19* qRT-PCR assay on whole liver specifically amplified human *KRT19*. 3 of 6 DDC-treated chimeric mice had robust *KRT19* induction. D) *KRT19* levels relative to human *LMNA* were only 9-to-285 fold lower (n=3) than human liver reference samples (n=2). E) RNA-sequencing of whole chimeric livers effectively separated human (blue) from mouse (red) transcripts, graphed as unique transcript-mapped reads per position across each UCSC gene model (3 examples shown). The *FAH* transcript in chimeric livers shows expected truncation of mouse *Fah* [exon5] and non-sense mediated decay but full length human FAH. F) Human mRNA levels of ductal progenitor genes were quantified relative to housekeeping gene *LMNA* in normal human liver (n=1), chimeric livers (n=6), and DDC injured chimeric livers (n=3)(mean ± SEM, *p <0.05, **p < 0.01, *** p<0.001).